Journal of the Nigerian Association of Mathematical Physics
Volume34,(*March, 2016*), pp 461 – 470

Resolution Analysis of Different Electrode Array on Synthetic Earth Models of Geological Relevance

Adeoti L.[1], Ishola K.S.[1], Imenvbore I.[1], Ojo A. O.[1], Adegbola R.B.[2] and Afolabi S.O.[1]

[1]Department of Geosciences, Faculty of Science, University of Lagos, Lagos, Nigeria
[2]Department of Physics, Faculty of Science, Lagos State University, Ojo, Lagos, Nigeria.

Abstract

This study compares the resolution capabilities of different electrode arrays in imaging 2-D earth models by employing the Finite difference modeling scheme. The software called RES2DMOD was used to generate 2-D synthetic models having a resistive block in a conductive environment with different resistivity values, three conductive blocks in a highly resistive environment and a high resistive dyke in conductive environment. The synthetic data were contaminated with 6% Gaussian noise and inverted using the RES2DINV inversion software. The reconstructed resistivity values reproduced from a block of 100 Ωm at a depth of 2.8 m by Dipole-dipole, Pole-dipole, Wenner-schlumberger and Wenner arrays are 94.1 Ωm, 90.9 Ωm, 77.8 Ωm and 46.7 Ωm respectively. For a dyke model with a resistivity of 500 Ωm, the inverted resistivity values are 355 Ωm, 312 Ωm, 281 Ωm, and 291 Ωm respectively. This shows that the dipole-dipole array recover a more accurate resistivity value of the block. However, the pole dipole array gives a higher resolution image at deeper depth when two blocks of different resistivity values in a conductive environment along a spread of 35 m. For the same structure, the dipole-dipole, pole-dipole, schlumberger and wenner arrays gave a depth estimates with variation of 9.12m, 13.6m, 7.88m and 6.75m from the true value. The study shows that dipole dipole gives best resolution for vertical structures such as dykes while the Pole-dipole seems more efficient for this same purpose at deeper depth. Also, Wenner array gives low resolution while investigating dipping structures. Schlumberger array was able to image sharp boundaries between two lithological units but gives poor results for dipping structures.

Key words: Finite difference method, synthetic model, RES2DMOD, RES2DINV, resolution

1.0 Introduction

The application of models in electrical methods of geophysical prospection is a vital tool in interpretation of electrical responses (i.e., resistivity, conductivity, and chargeability) over target of different shapes, sizes and dimensions [1]. Amongst the earliest studies in geophysics involves the use of resistivity methods in which apparent resistivity responses using theoretical models were carried out [2, 3]. Also, the techniques have been extended with success to mineral investigation and the relative advantages and limitations of different electrode being documented[4-7].

Geoelectrical surveying techniques have become a popular choice for shallow subsurface investigations and has been applied with great success to solve hydrogeological [8, 9], geological [10, 11], engineering and environmental problems [12-14]. The most widely used of these methods is Electrical Resistivity Tomography (ERT). The importance of the sampling density in determining the resolution of electrode array configuration was carried out by [15,16]. Recent studies have shown that by using a large set of well-distributed and spaced measurements, it is generally possible to obtain a reliable 2D/3D resistivity images of the subsurface with good resolution [17-25].

Two strategies for obtaining the maximum spatial resolution in electrical resistivity tomography surveys using a limited number of four-electrode measurement configurations by employing model resolution matrices and linear independence of the Jacobian matrix elements, the first method produces results that are nearer to optimal, but the second is several orders of faster magnitude[26].The resolution of different types of geological structure in the subsurface varies with different types of electrode configuration.

Corresponding author: Adeoti L., E-mail:lukuade@yahoo.com, Tel.: +2348034739175

The sensitivity of different kind of electrode array to noise which contaminates geoelectric data varies from one configuration to another thereby influencing the resolution of the model. A study of crosshole resistivity imaging using somespecifiedelectrodeconfigurations was carried outand concluded thata comprehensive comparison of the imaging abilities of the different electrode array is needed to understand the geoelectric response over different geologic structures for practical imaging applications [27]. This suggests that additional research work is required to understand the use of these arrays so that their characteristics can be more fully understood and explored. This will also help us understand the spatial resolutions and the noise sensitivitiesofthese different electrodearraysforfieldworkdesignand aid datainterpretation. In this way, we can predict which features of the earth model can be resolved and which details cannot be resolved from the imaging surveys using these electrode arrays. Decision prior to field survey on the best electrode array that could be used with a view to imaging the feature of interest with high resolution under minimal data gathering is taken. It follows therefore that time could be saved and cost of geophysical survey in obtaining optimum results reduced.

In this study, four electrode configurations namely: Wenner, Wenner-Schlumberger, Pole-dipole and Dipole-dipole arrays for imaging four different synthetic models of geological relevance were considered. We assessed their resolution ability by comparing recovered model parameter with the true model parameter.

1.1 Basic Theory

Solutions to the forward problem require that we derive a theoretical response based on a given set of input parameters, using the appropriate equations that relate the model to the data. For electrical resistivity method, this physical law is governed by a second-order differential equation (Poisson's equation) which can be solved analytically or approximately using numerical methods. For arbitrary resistivity distribution, the Finite Difference (FD) or Finite Element (FE) techniques are often used to solve the Poisson's equation in multidimensional cases. For a 2-D earth model, it is assumed that the current is suppliedto the ground by means of a pair of infinite lineelectrodes, extending at right angles to the directionof the measurement profile and there is no change in the conductivity distribution along the y-direction. Therefore the resistivityproblem can be treated as purely 2-D and can be solved easily by a finite-differenceevaluation of the potential field and apparent resistivity curves [28]. The flow of steady electric current in a non-uniform medium containing a current source is governedby the equation below [29]:

$$-\nabla.\left(\frac{1}{\rho(x,y,z)}\nabla v(x,y,z)\right) = \frac{\partial Q(x,y,z)}{\partial t} \qquad (1.1)$$

When the system represented by (Equation 1.1) is restricted to two dimensions (x, z), then it becomes

$$\frac{\partial}{\partial x}\left(\frac{1}{\rho(x,z)}\frac{\partial v}{\partial x}\right) + \frac{\partial}{\partial z}\left(\frac{1}{\rho(x,z)}\frac{\partial v}{\partial z}\right) + q(x,z) = 0 \qquad (1.2)$$

$$\frac{\partial Q(x,y,z)}{\partial t} = q(x,z)$$

Where **ρ** is the resistivity of the medium [ohm-m], ***v*** is the electric scalar potential [volt], **q** is the charge density [Ampere m^{-2}].

The FD scheme was first developed in [29] and later improved upon in [30]. Using this scheme, the potential distribution in the 2D transformed potential (Equation 1.2) can be solved by the FD algorithm according to the discretization-by-area method developed in [30]. In this case, the earth is discretized into domains using irregular mesh of nodes which divides the earth into rectangular blocks each having homogeneous and isotropic resistivity. The semi infinite medium was made finite by introducing an artificial boundary and dividing the mesh into a number of rectangular cells as shown in Figure 1 so as to reflect the changes in resistivity distribution and to allow for reliable estimation of the potential difference variations across the region. Each of these points is called an element of the discretized medium and represents a vertical cross-section of the ground**.** The calculation of the potential distribution cross the discretized semi-infinite rectangular grids is solved by Finite Difference Method (FDM).

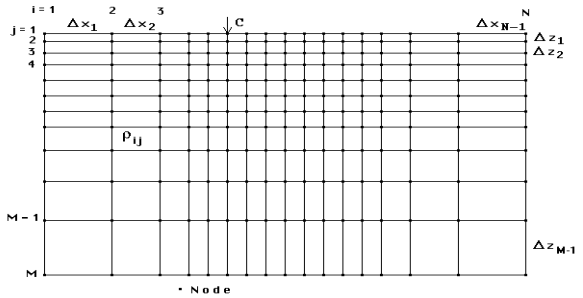

Figure 1: 2-D Finite Different Rectangular Mesh

An illustration of this method is shown in Figure 2. Suppose the element P represents the location of a current electrode supplying **I** amperes into the subsurface such that its neighboring elements are denoted by E, W, N. and S. Since the point P represents the shaded area *abcd*, the current density q_p due to the electrode at P is given as:

$$q_p = \frac{I}{(Areaabcd)} \quad (1.3)$$

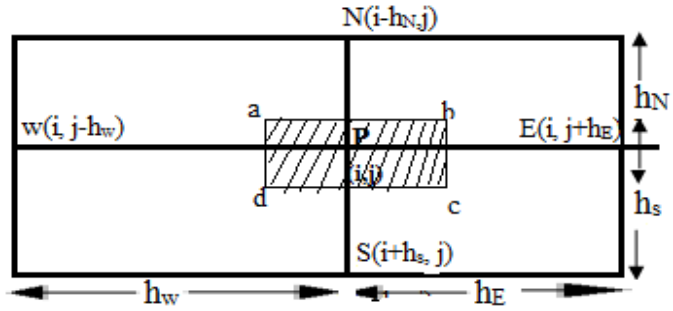

Figure2: An Element P Representing a Current Source in a Discrete Model [29]
Hence, the approximated potential difference *v*(i,j) at point P using central difference formula [31] is

$$\left(\frac{\partial v}{\partial x}\right)_{i,j} = \frac{v_{i,j+h_{E/2}} - v_{i,j-h_{W/2}}}{h_E + h_w/2} \quad (1.4)$$

Also at point (i,j-$h_{w/2}$) is given

$$\left(\frac{1}{\rho}\frac{\partial v}{\partial x}\right)_{i,j-h_{w/2}} = \left(\frac{1}{\rho}\right)_{i,j-h_{w/2}} h_w^{-1}\left(v_{i,j} - v_{i,j-h_w}\right) \quad (1.5)$$

Also, at point (i,j+$h_{E/2}$)

$$\left(\frac{1}{\rho}\frac{\partial v}{\partial x}\right)_{i,j+h_{E/2}} = \left(\frac{1}{\rho}\right)_{i,j+h_{E/2}} h_E^{-1}\left(v_{i,j+h_{E/2}} - v_{i,j}\right) \quad (1.6)$$

This represents the solution to the Jacobian Matrix in trying to approximate the non-linear of the inversion scheme. The resistivities are discretized and interpreted as averages center of each cell. In other words, the subsurface resistivity can be obtained from the second order differential equation after performing some iterations.

2.0 Methodology

2.1 Modeling Procedure

Synthetic data computed for generic earth models using the RES2DMOD [32] forward modeling software were contaminated with 6% Gaussian noise prior to inversion. This became necessary in order to reflect field conditions. Synthetic data were obtained using Wenner (Wen), Wenner-Schlumberger (WenSch), pole-dipole (PdP) and dipole-dipole (DpDp) arrays and subsequently inverted the synthetic dataset with the RES2DINV [32] inversion software. The inversion algorithm that is commonly used for regularization based on the least-squares optimization scheme is the smoothness-constrained or L_2- norm method [33]. It gives optimal results where the subsurface geology exhibits a smooth variation [34]. In situation where a sharp transition in the subsurface resistivity is expected (for instance a dyke), this scheme tends to smear out the boundaries. Another optimization scheme is the blocky or L_1-norm that tends to produce models with regions that is piecewise constant and separated by sharp boundaries [35]. For this study, the L_1- norm optimization method was adopted because it allows models with sharp variations in resistivity which is a good choice when geological discontinuities are expected [36]. The synthetic models used in this study represent some geological structures useful for groundwater, archaeological and environmental studies. Summary of the parameters adopted for the inversion processes is shown in Table 1.

Table 1: Summary of the Parameters and information used for the 2D Resistivity Inversion (Modified After [37])

Initial Damping Factor	0.25
Minimum Damping Factor	0.015
Convergence Limit	1.00
Minimum Change In Absolute Error	
Number Of Iterations	3-7
Jacobian Matrix Is Recalculated For First Two Iterations	
Increase Of Damping Factor With Depth	1.0500
Robust Data Inversion Constrain Is Used With Cut Off Factor	0.05
Robust Model Inversion Constrain Is Used With Cut-Off Factor	0.005
Extended Model Is Used	
Effect of Side Blocks Is Not Reduced	
Normal Mesh Is Used	
Finite Difference Method Is Used	
Number of Nodes Between Adjacent Electrodes is 4	
Logarithm of Apparent Resistivity Used	
Reference Resistivity used is the average of Minimum and Maximum Values	
Gauss - Newton Optimization Method	

2.2 Model Parameterization

2.2.1 Single Resistive Block Model

The first model is a resistive block prism of 100 Ω m buried in a surrounding background of low resistivity value of 10 Ωm half space homogenous medium (Figure 3).The block prism was positioned between the 15th and 20th electrodes at a depth of 1.2 m. This model depicts block slab for drainage system allowing water flow in less resistive medium clay.

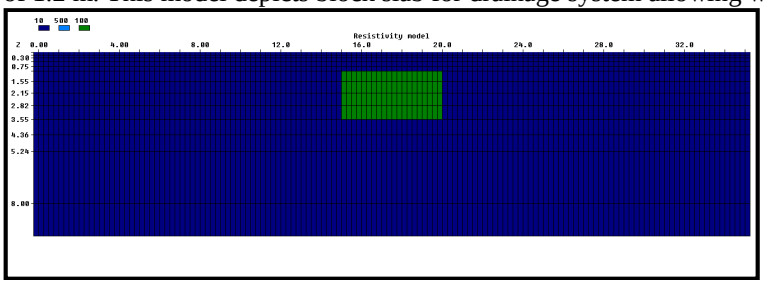

Figure 3: Generic Model for a Resistive Block

2.2.2 Double Resistive Block Model

This model comprised two blocks with resistivity estimations of 300 Ωm and 500 Ωm for the left and right block separately embedded in a homogeneous medium with resistivity of 10 Ωm (Figure 4). The left block was situated between the 10th and 14th electrodes with thickness of 2.81 m while the right block was set in between 20th and 24th electrodes with a thickness of 1.17 m.

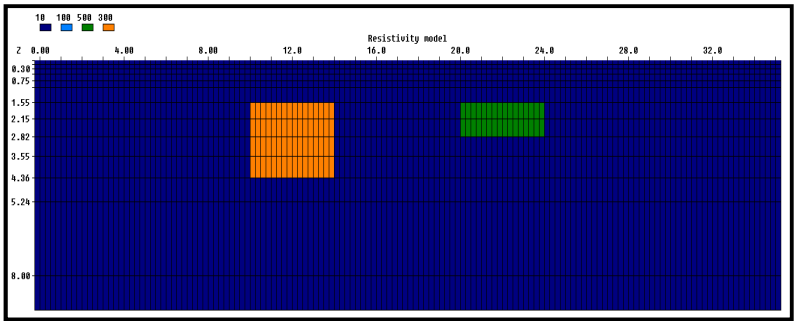

Figure 4: Generic Model for Double Resistive Block.

2.2.3 Three Conductive Block Model

Three blocks of different dimensions and resistivity of 100 Ωm were embedded in a conductive homogenous half space with resistivity of 10 Ωm (Figure 5). The thicknesses of the block 1, 2, 3 are 1.59, 4.13, and 3.96 respectively

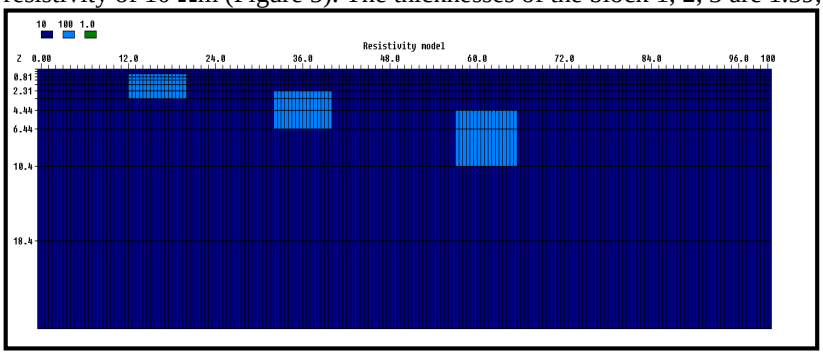

Figure 5: Generic model of Three Resistive Blocks.

2.2.4 Dipping Dyke Model

A dipping dyke with resistivity of 500 Ωm overlain by a layer of 300 Ωm, across a homogeneous medium with resistivity of 100 Ωm was simulated representing a geological model of saturated fractured zone in the subsurface (Figure 6). The location of dyke lies between 140-165 m along horizontal distance.

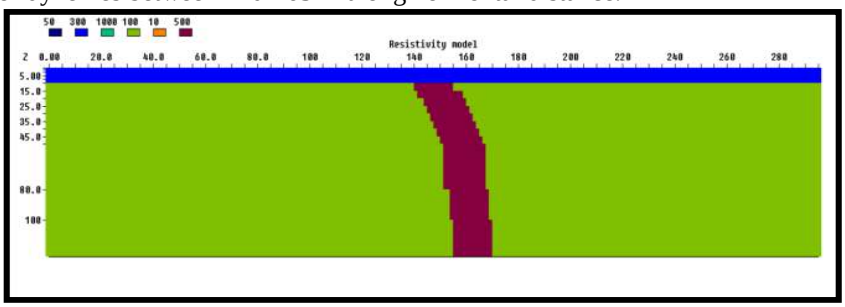

Figure 6: Generic Model of Dipping Resistive Dyke

3.0 Results and Discussion

The inverted 2-D resistivity models from the inversion software RES2DINV [32] are shown in Figures 7 to 10. Also, Tables 2 and 3 present the recovered resistivity of the models in comparison to the true models and the estimated pseudo-depth of the inverted models respectively. For a resistive block model, the inverted model parameters using Wenner, Wenner-Schlumberger, Dipole-Dipole and Pole-Dipole arrays with true resistivity and thickness of 100 Ω m and 2.55 m buried in a homogenous environment of resistivity 10 Ω m (Figure 2) are 46.7 Ωm, 77.8Ωm, 94.1Ω m and 90.0 Ω m respectively as shown in Figure 7. The inverted model parameter using Dipole-dipole array (Figure 7) gave the closest value to the true model parameter and that of the background environment while the inverted resistivity image from Wenner array gave the poorest representation of the block model since the block model is associated with the least resistivity (Table 2). Moreso, for the block model, the recovered depth ranges from 6.75 m for Wenner array to 13.6 m for pole-dipole array (Table 3). For this model, it was observed that dipole-dipole followed by Wenner-Schlumberger and Pole-Dipole almost gave a replica of the true model whereas Wenner array gave the least representatives of the true model.

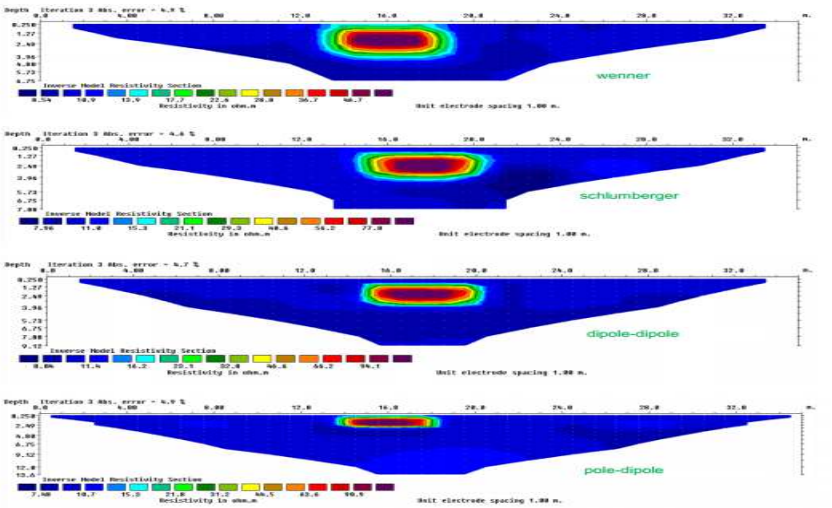

Figure 7:2-D inverse resistivity model of Single Resistive block images for (a) Wen (b) Sch (c) DpDp (d) PdP

Table 2: Summary Of Reconstructed Resistive For Models

Model		True Res. (Ωm)	Reconstructed Resistivity (Ωm)			
			Wenner	Wenner-Schlumberger	Dipole-Dipole	Pole-Dipole
One Block		100	46.7	77.8	94.1	90.9
Two Blocks	Block 1	300	38.7	82.4	98.7	145
	Block 2	500	30.4	82.4	95.0	140
Three Blocks	Block 1	10	6.12	6.01	8.96	4.68
	Block 2	10	10.5	8.81	12.3	7.07
	Block 3	10	30.5	12.9	17.0	10.7
Dyke		500	291	281	355	312

Table 3: Pseudo-Depth of the Inverted Model

Model	True depth (m)	Wenner	Wenner-Schlumberger	Dipole-Dipole	Pole-Dipole
One Block	1.2	6.75	7.88	9.12	13.6
Two Blocks	1.55	6.75	7.88	9.12	13.6
Three Blocks	0.5, 2.31, 4.44	19.6	19.6	42.5	42.5
Dyke	10	52.4	59.9	110.2	110.2

For the double resistive block model with true resistivity values of 300 Ωm and 500 Ωm embedded in a homogenous medium 10Ωm, the inverted resistivity values range between 38.7Ωm to 145Ωm as shown in Figure 8 indicating that the true resistivity values are underestimated. The reconstructed resistivity values for the first and second blocks show that pole-dipole gave the closest resistivity values of 140 and 145 Ω m respectively whilst the reconstructed resistivity of Wenner array (Table 2) gave the poorest representation of the true model. The estimated depth of burial of the recovered blocks like the single block ranges from 6.75m for Wenner to 13.6m for pole-dipole array (Table 3).

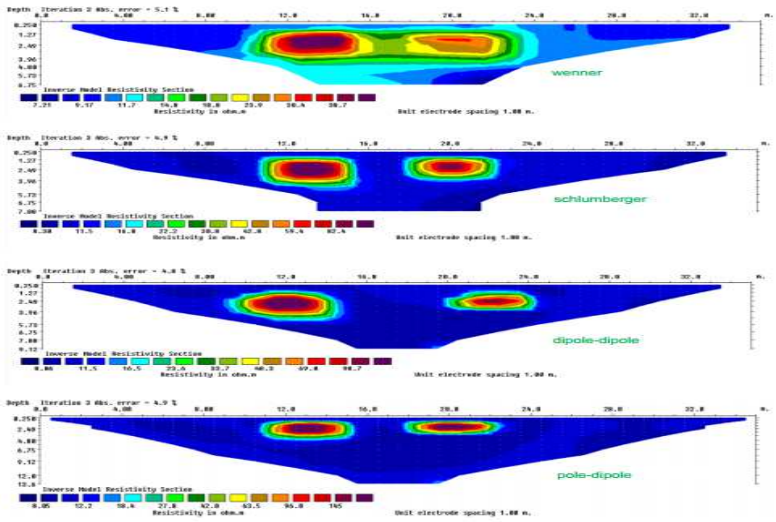

Figure 8:2-D inverse resistivity model of two blocks images for (a) Wen (b) Sch (c) DpDp (d) PdP

For the three conductive blocks model, the reconstructed resistivity values for each electrode configuration are shown in Figure 9 while the reconstructed resistivity values in comparison to the true model resistivity is presented in Table 2. Also, it was observed that the reconstructed resistivity values for the three blocks are underestimated. This may be as a result of the influence of the background resistivity on the resistivity of the individual blocks. However, the inverted resistivity value of the three blocks for Dipole-dipole array inversion image is closer to the true resistivity values of the blocks while the inverted image of the Wenner array gave the least values expect for the third block of resistivity 500 Ω m (Table 2). Also, for this model, it was observed that the reconstructed blocks appear deeper than the true depth of the model with depth variation from 19.6 m for the Wenner and Wenner-Schlumberger arrays to 42.5m for both dipole-dipole and pole-dipole arrays (Table 3). The failure of the reconstructed models to be located exactly at the position of the true models could be due to model inadequacy a persistent problem in inversions as model of the earth will always be inadequate especially the actual geological structures are complex [7].

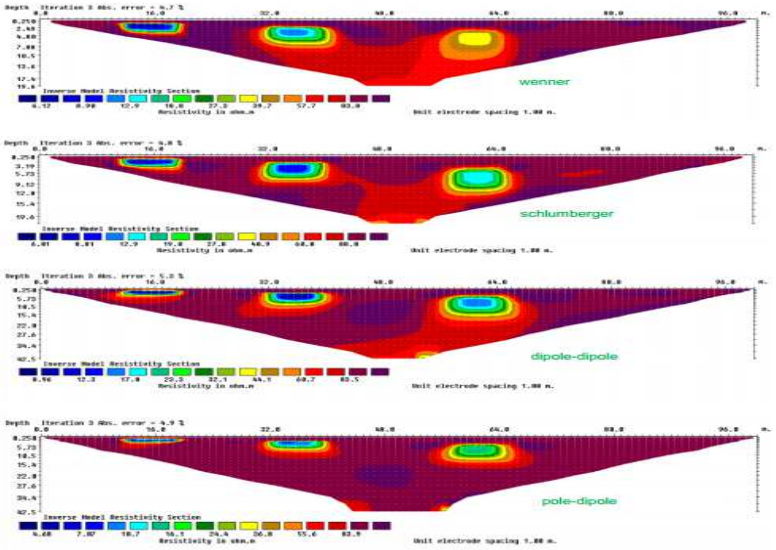

Figure 9:2-D inverse resistivity model of Three blocks for (a) Wen (b) Sch (c) DpDp (d) PdP

The inverted model for the dipping dyke with a true resistivity of 500+

+ Ωm overlain by a resistive top layer of 300 Ωm, in a background of 100 Ωm is shown in Figure 10. The reconstructed resistivity values for the dipole-dipole, pole-dipole, Wenner-Schlumberger and Wenner arrays are 355 Ωm, 312 Ωm, 281 Ωm, and 291 Ωm respectively. These range of reistivity indicate that the true model resistivity of 500 Ωm was underestimated (Table 2). The recovered resistivity for the dipole-dipole array image give the closest resitivity to the model true resistivity. This is followed by the pole- dipole array while a poor reconstructed image was obtained for the Wenner array. Although the Wenner and Wenner-schlumberger produce a clear image of the dike, both have distortions on each side of the dyke.

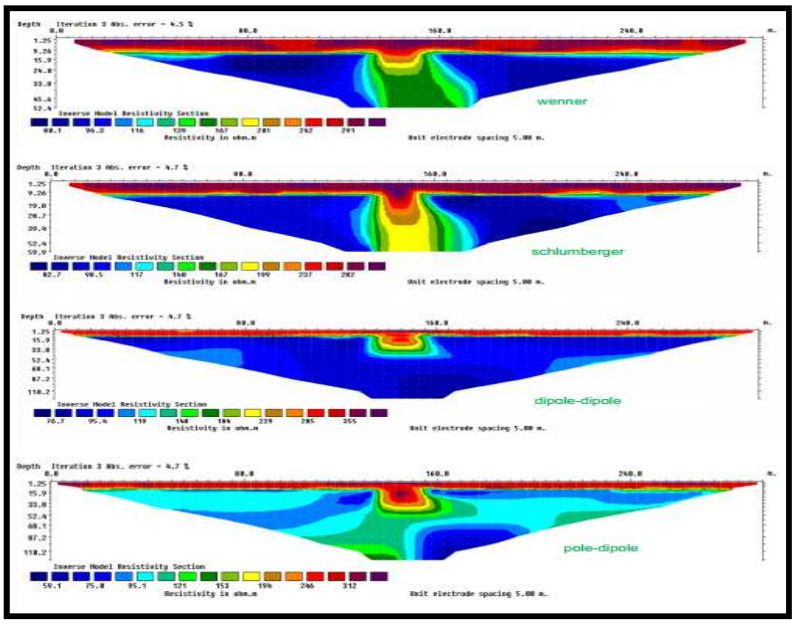

Figure 10:2-D inverse resistivity model of Dipping Dyke for (a) Wen (b) Sch (c) DpDp (d) PdP

4.0 Conclusion

2-D resistivity modeling employing four electrode configurations has been carried out on different synthetic models of geological significance in order to compare the imaging capabilities of these different arrays. This study reveals that all the electrode arrays considered in this study are able to delineate the contact between two geologic units where ever the resistivity contrast is high. However, the accuracy of the position of the vertical (dyke) structure differs for different arrays. Thedipole-dipolearraygivesthebestrepresentation for all models considered and gave themostdetailed imagesespeciallyforthedetectionofverticalstructures such as dyke intrusions.ThePole-dipole array also gives good results comparable to the dipole-dipole arrayinthe synthetic modelling.The recovered images using the Wenner array usually has alowresolution which makes itnon-efficient for detailedinvestigationofdipstructures. The Wenner-Schlumbergerarray generally givesagoodresolutionbutgives a poorresult forimaging dipping structures.

5.0 References

[1] Coggon, J.H. (1971). Electromagnetic and electrical modeling by the finite element method. Geophysics, 36: 132-155.

[2] Hummel, J.N. (1932). A theoretical study of apparent resistivity in surface potential methods. Geophysical Prospecting, 97: 392-427.

[3] Van Nostrand, R.G., and Cook, K.L. (1966). Interpretation of resistivity data. U.S.G.S. Professional Paper No. 499

[4] Loke, M.H. (2001). Electrical imaging surveys for environmental and engineering studies: a practical guide to 2D and 3D surveys, 62 pp. http://www.geoelectrical.com

[5] Dahlin, T., Sjödahl, P., and Zhou, B. (2004). 2.5D resistivity modeling of embankment dams to access influence from geometry and materials properties. GEOPHYSICS, 71, 3; P. G107–G114, 10.1190/1.2198217.

[6] Aizebeokhai, A. P., Olayinka, A.I., and Singh, V.S. (2010). Application of 2D and 3D geoelectrical resistivity imaging for engineering site investigation in a crystalline basement terrain, southwestern Nigeria. Environ Earth Sci. DOI: 10.1007/s12665-010-0464-z.

[7] Ishola, K., S., Nawawi, M. N. M., Abdullah, K., Sabri,A., I., A and Adiat, K.,A (2014). Assessment of the Reliability of Reproducing Two-Dimensional Resistivity Models using an Image Processing Technique. Springerplus, 3:214.DOI: 10.1186/2193-1801-3-214

[8] Flathe H. (1955). Possibilities and Limitations in Applying Geoelectrical Methods to Hydrogeological Problems in the Coastal Areas of Northwest Germany. Geophysical Prospecting, 3: 95–110

[9] Dahlin, T. and Owen, R. (1998). Geophysical Investigations of Alluvial Aquifers In Zimbabwe. Proceedings of The Iv Meeting Of The Environmental and Engineering Geophysical Society (European Section), September, Barcelona; 151–154

[10] Caglar, I. And Duvarci E. (2001). Geoelectric Structure Of Inland Area Of Go ¨Kova Rift, Southwest Anatolia And Its Tectonic Implications. Journal of Geodynamics, 31: 33–48.

[11] Atzemoglou A., Tsourlos P. and Pavlides S. (2003). Investigation Of The Tectonic Structure Of The NW Part Of The Amynteon Basin (NW Greece) By Means Of A Vertical Electrical Sounding (VES) Survey. Journal of the Balkan Geophysical Society, 6(4): 188–201.

[12] Rogers R.B. and Kean W.F. (1980). Monitoring Ground Water Contamination at A Fly Ash Disposal Site Using Surface Resistivity Methods. Ground water, 18(5): 472–478.

[13] Van P.V., Park S.K., and Hamilton P. (1991). Monitoring Leaks From Storage Ponds Using Resistivity Methods. Geophysics, 56: 1267–1270.

[14] Ramirez., A, Daily, W., Binley, A., and Labrecque, D. (1996). Tank Leak Detection Using Electrical Resistance Methods. Symposium on the Application of Geophysics To Engineering And Environment, Keystone, Co; 28 April–1 May.

[15] Dahlin, T. and Loke, M. H. (1998). Resolution of 2D Wenner Resistivity Imaging As Assessed by Numerical Modelling. Journal of Applied Geophysics, 38(4): 237- 249

[16] Olayinka, A. I., and Yaramanci, U. (2000). Assessment of the Reliability of 2d Inversion of Apparent Resistivity Data: Geophysical Prospecting, 48: 293–316.

[17] Daily, W. and Owen, E. (1991). Cross-borehole Resistivity Tomography. Geophysics, 56(8): 1228-1235.

[18] Park, S. K. and Van, G. P. (1991). Inversion of Pole-Pole Data for 3-D Resistivity Structure Beneath Arrays Of Electrodes. Geophysics, 56(7): 951-960.

[19] Shima, H. (1992). 2-D And 3-D Resistivity Image Reconstruction Using Crosshole Data. Geophysics, 57(10): 1270-1281.

[20] Sasaki, Y. (1994). 3-D Resistivity Inversion Using The Finite-Element Method. Geophysics, 59(12): 1839-1848.

[21] Loke, M.H. and Barker, R. D. (1995). Rapid Least Squares Inversion of Apparent Resistivity Pseudo-Sections By A Quasi-Newton Method. Geophysical Prospecting, 44:131–152.

[22] Loke, M. H., and Barker, R. D. (1996). Practical Techniques for 3d Resistivity Surveys and Data Inversion. Geophysical Prospecting, 44(3): 499-523.

[23] Labrecque D, Miletto M, Daily W, Ramirez A and Owen E (1996). The Effects of Noise on Occam's Inversion of Resistivity Tomography Data, Geophysics, 61(2):538–548.

[24] Chambers, J., Ogilvy, R., Meldrum, P. And Nissen, J. O. H. A. N. (1999). 3D Resistivity Imaging of Buried Oil- and Tar-Contaminated Waste Deposits. European Journal of Environmental and Engineering Geophysics, 4(1): 3-16.

[25] Dahlin, T. and Zhou, B. (2004). A Numerical Comparison of 2-D Resistivity Imaging With10 Electrode Arrays. Geophysical Prospecting, 52 (5): 379–398

[26] Wilkinson, P.B., Meldrum, P.I., Chambers, J.C., Kuras, O. And Ogilvy, R.D. (2006). Improved Strategies For The Automatic Selection Of Optimized Sets Of Electrical Resistivity Tomography Measurement Configurations. Geophysical Journal International, 167: 1119–1126.

[27] Zhou, B. and Greenhalgh, S. A. (2000). Cross-Hole Resistivity Tomography Using Different Electrode Configurations. Geophysical Prospecting, 48(5): 887-912.

[28] Gerald, C., F., and Wheatley, P., O., (1997). Applied Numerical Analysis. Addison Westley Longman, Inc

[29] Irshad, R., M.(1976). Finite Difference Resistivity Modeling for Arbitrarily Shaped Two Dimensional Structures. Geophys prosp. 41: 62-78.

[30] Dey, A., Morrison, H.F., (1979). Resistivity modeling for arbitrarily shaped two- dimensional structures. Geophysical Prospecting, 27: 106–136

[31] Smith, G. D.. (1965). Numerical Solution of Partial Differential Equations: New York Oxford University Press.

[32] Loke, M.H. (2004). User's Manual for RES2DMOD and RES2DINV Software. Geotomo Software, pp: 128.

[33] deGroot-Hedlin, C. and Constable, S., (1990). Occam's Inversion to Generate Smooth, Two Dimensional Models Form Magnetotelluric Data. Geophysics.55: 1613-1624.

[34] Loke, M.H., Chambers, J.E., Rucker, D.F., Kuras, O. and Wilkinson, P.B. (2013). New Developments in the Direct-Current Geoelectrical Imaging Method. Journal of Applied Geophysics, 95: 1 35–156.

[35] Ellis, R.G. & Oldenburg, D.W., (1994). The pole–pole 3-D DC-resistivity inverse problem, a conjugate gradient approach, Geophys. J. Int., 119: 187–194.

[36] Seaton, W. and Burbey, T. J. (2002). Aquifer Characterization in the Blue Ridge Physiographic Province Using Resistivity Profiling And Borehole Geophysics. Journal Of Environmental And Engineering Geophysics 5(3): 45–58

[37] Martorana R, Fiandaca G, CasasPonsati A, Cosentino PL (2009). Comparative Tests on Different Multi-Electrode Arrays using Models in Near-Surface Geophysics. J Geophys Eng 6:1–20.